Impact of Big Vehicle Shadowing on Vehicle-to-Vehicle Communications

Hieu Nguyen, Xu Xiaoli, Md. Noor-A-Rahim, Yong Liang Guan, Dirk Pesch, Hong Li, and Alessio Filippi

***Abstract*—Vehicle to vehicle (V2V) communications using dedicated short-range communications (DSRC) are considered a promising technology for enhancing road safety. However, in V2V communications, passenger cars suffer from obstruction of bigger vehicles such as buses or trucks. Based on our measurement, a big vehicle can cause a signal loss from 10 to 15 dB due to shadowing. This results in a shorter communication range and reduces the safety message dissemination capability. In this paper, we analyze the impact of shadowing caused by multiple big vehicles on the V2V communication of passenger cars. We propose a model that takes into account both geometric and stochastic shadowing of multiple big vehicles. In order to cope with the physical size of vehicles and safety distance between them in the real world, we propose to use a repulsive point process called hardcore repulsive Poisson point process (PPP) to model the locations of vehicles. Generating procedure and some basic properties of this process are introduced. Based on the proposed model, we derive the average length of the shadow region and the shadowing loss caused by multiple big vehicles. We show that when the number of big vehicles increases from 10% to 80% of total vehicles in one lane, the shadow region increases from 50 m to 450 m on the road. Furthermore, the shadowing loss causes the relative number of cars within communication range of a typical car to reduce from 90% to between 15% and 50%, depending on whether the big vehicles are in the same or the adjacent lane of the consider car. We analyse the packet collision probability while taking into consideration the big vehicle shadow region and observe significant packet collisions without dedicated bus lanes.**

***Index Terms*—IEEE 802.11p, DSRC, V2V communications, LOS, OLOS, shadowing, Poisson point process, repulsive point process.**

Manuscript received November 1, 2019; revised March 6, 2020; accepted May 3, 2020. Date of publication May 14, 2020; date of current version July 16, 2020. This work was supported in part by A*STAR under its RIE2020 Advanced Manufacturing and Engineering (AME) Industry Alignment Fund – Pre Positioning (IAF-PP) (Grant No. A19D6a0053), in part by the European Union's Horizon 2020 Research and Innovation Programme under the Marie Sklodowska-Curie EDGE Co-FUND Grant 713567, and in part by Science Foundation Ireland under CONNECT Centre Grant 13/RC/2077. The review of this article was coordinated by Prof. T. Kurner. *(Corresponding author: Md. Noor-A-Rahim.)*

Hieu Nguyen and Yong Liang Guan are with the School of Electrical and Electronic Engineering, Nanyang Technological University, Singapore 639798, Singapore (e-mail: nguyenth@ntu.edu.sg; eylguan@ntu.edu.sg).

Xu Xiaoli is with the National Mobile Communications Research Laboratory, School of Information Science and Engineering, Southeast University, Nanjing 210096, China (e-mail: xiaolixu@seu.edu.cn).

Md. Noor-A-Rahim and Dirk Pesch are with the School of Computer Science and IT, University College Cork, Cork T12 XF62, Ireland (e-mail: m.rahim@cs.ucc.ie; d.pesch@cs.ucc.ie).

Hong Li and Alessio Filippi are with the NXP Semiconductor, Eindhoven 5656 AG, The Netherlands (e-mail: hong.r.li@nxp.com; alessio.filippi@nxp.com).

Digital Object Identifier 10.1109/TVT.2020.2994407

I. Introduction

VEHICLE-to-everything (V2X) communication is an important part of intelligent transport systems (ITS). Dedicated Short-Range Communications (DSRC) [1], [2] is a strong candidate for V2X communications along with LTE-V2X communications [3], [4]. DSRC uses the IEEE 802.11p standard which is designed for vehicular ad-hoc networks. A vehicle equipped with an IEEE802.11p on-board unit (OBU) will exchange information with other vehicles or with infrastructure equipped with roadside units (RSUs). The vehicle information related to safety application such as locations, speed, heading, etc., extracted from Global Navigation Satellite System (GNSS) system on vehicle, and vehicle type, break condition are organized into short messages follow the J2735 SAE standard format [5] to be broadcasted to other vehicles [6], [7]. Other vehicles' information can be used to evaluate the traffic situation and generate early warning messages to the driver if necessary. Many situations can make use of vehicle information such as Electronic Emergency Brake Light (EEBL), Forward Collision Warning (FCW), Blind Spot Warning (BSW), Lane Change Warning (LCW), Intersection Movement Assist (IMA), Do Not Pass Warning (DNPW) and Left Turn Assist (LTA) [8]. Vehicles can also receive support information from the infrastructure through RSUs such as Curve Speed Warning (CSW), Work Zone Warning (WZW) and In-Vehicle Signal Phase and Timing (SPaT). All these messages will help to enhance road safety.

The capability of short message dissemination of a vehicle depends on the link quality of the V2V communications. Due to low position of antennas on vehicles, the V2V communication link can be heavily degraded by large obstructions such as a bus or truck. Many existing performance analysis of V2V communications have overlooked the impact of shadowing due to big vehicle obstruction [9]–[11]. Recently, it was shown in [12] and [13] that a big vehicle can block the line of sight (LOS) component of V2V communications and cause significant attenuation of the received signal. The authors in [12] report that a single bus obstruction generally causes 15–20 dB loss in the received signal passing by it, which was measured in a campus environment. In another measurement, Abbas *et al.* find that the obstruction loss is about 8.6–10 dB [13]. They add this loss to network simulations to make the scenario more realistic [13]. The blockage effect of a big vehicle on a V2I link at an intersection is introduced with a semi closed-form expression in [14]. However, the authors do not use the stochastic model for vehicle and propose any model for a V2V link. In [15], the

authors provide measurement based analysis for multiple link shadowing effects. Whereas in [16]–[18], the authors have proposed an empirical model of shadowing by using data from aerial photography of Portuguese highways near the city of Porto to fit their model. This model has been used in [19] to evaluate and improve the broadcast safety information. However, the above mentioned works focus on the empirical model of shadowing of car based on static photography, without considering the vehicle traffic model.

For the analysis of vehicular networks in [9]–[11], [13], [20]–[22], PPP is a commonly adopted model for vehicles due to its mathematical tractability [23]. However, vehicles have a physical size and cannot be considered as an ideal point. Furthermore, a vehicle has to keep a safe distance to other vehicles and objects, which means it exhibits the behavior of repulsive objects. A better way to model vehicles would be by a repulsive point process such as a Matérn hardcore point process type I, II, and III [24]–[26], a Ginibre point process [27]–[30] or a Poisson Cox point process [31]. All of them are complex processes to model vehicle traffic and are not always tractable. To model vehicles on a straight road, we propose to add a safety space between two consecutive vehicles which were originally generated by a PPP. This tractable process is similar to 1-dimensional Matérn hardcore point process, which is hence referred to as a hardcore repulsive PPP. This process describes a vehicle on a straight road with a minimum separation between two adjacent vehicles.

In this paper, we propose a comprehensive model that incorporates multiple obstructions of big vehicles on a highway based on measured data. The key findings of our research include

- **Calculation of the shadow region cast by big vehicles on the road:** Multiple big vehicles will cast a shadow region onto other vehicles. The shadow region length for each lane on the road is analyzed with respect to both geometric and stochastic location for a conventional passenger car and a big bus in different scenarios.
- **Introduction of a repulsive point process to model vehicle locations on the road where vehicles have to keep a safety distance to other vehicles:** In the analysis, we use the hardcore repulsive PPP to model the vehicle location. We propose a generating procedure and derive the key parameters and distributions of this hardcore repulsive point process. These results are useful for both simulation and analysis that aim to model realistic vehicle locations on the road.
- **Calculation of the communication link quality degraded by big vehicle shadowing:** We also analyze the effect of big vehicle shadowing on the signal degradation of a V2V communication link. Specifically, the path-loss and shadowing loss are used to derive the link quality between a target vehicle to other vehicles within the region of interest.[1] The result shows that when the number of big vehicles is large, the quality of the physical layer link can reduce significantly, dropping from 100% to 15%. We further analyse the impact of bus shadowing on the packet collision rate and show that the packet collision rate is severe in a scenario without bus lanes compared to one with bus lanes.

The rest of this is organized as follows, Section II presents the V2V channel models with and without big vehicle shadowing based on our measurement. Section II also illustrates the geometric shadowing for different relative locations of a conventional passenger car and a big vehicle such as a bus. The shadowing effect is further investigated in Section III using a stochastic geometry approach where the locations of a vehicle are randomly distributed. Section IV analyzes the hidden node problem caused by shadowing. Simulations are carried out and their results are presented and discussed in Section V. Finally, this paper is concluded in Section VI.

II. V2V Channel Characterization With Big Vehicle Shadowing

A. Big Vehicle Shadowing

A V2V channel is characterized by several statistical metrics such as path-loss, fading statistics, Doppler spread, and delay spread. When a big vehicle is located between smaller vehicles, it may block the signal from the transmitter to the receiver. The attenuated received signal causes degradation in the communication performance.

In this paper, we consider a path-loss model, which is a function of distance between the transmitter and the receiver. Fluctuations in the received signal strength at large distances (more than 10 times the wavelength) are called large scale fading. Large scale fading with a relative received signal strength expressed in the dB scale is usually characterized by a Gaussian random variable with zero mean and variance of σ^2, denoted by X_σ. Specifically, the path-loss is expressed as a function of distance d as

$$PL(d) = PL_0 + 10n\log_{10} d + X_\sigma, \tag{1}$$

where PL_0 (in dB) is the pass loss at a reference distance d_0 (greater than 10 times the wavelength), d is the distance between Tx and Rx, n is the path-loss exponent, and X_σ represents the large scale fading. [2]

In V2V communication, due to the low position of the Tx and Rx antennas, the one slope model shown above is replaced by a dual-slope model where there are two path-loss exponents n_1 and n_2 instead of one n. The dual-slope model is expressed as

$$PL(d) = \begin{cases} PL(d_0) + 10n_1\log_{10}\frac{d}{d_0} + X_{\sigma_1} & d \le d_c \\ PL(d_0) + 10n_1\log_{10}\frac{d_c}{d_0} & \\ \quad +10n_2\log_{10}\frac{d}{d_c} + X_{\sigma_2} & d > d_c \end{cases}, \tag{2}$$

where d_c is the break point distance. In [32], d_c is considered to be the point where the first Fresnel zone touches the group,

[1]The target vehicle is the transmitting vehicle at the origin, and all other vehicles on the road are considered as potential receivers. The performance metrics (e.g., shadow region) are used for evaluating the receiving quality of other vehicles from this target vehicle. The target vehicle is assumed to be in the center of a circle with radius of region of interest, which is the transmission range of the target vehicle in the absence of bus shadowing.

[2]For simplicity, the small scale fading is neglected in this paper.

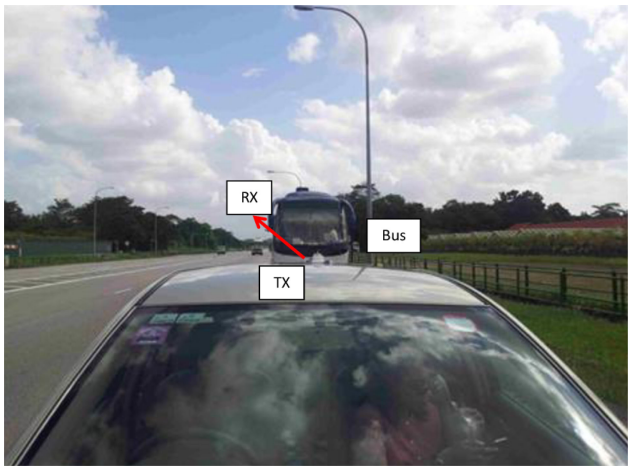

Fig. 1. Measurement setup.

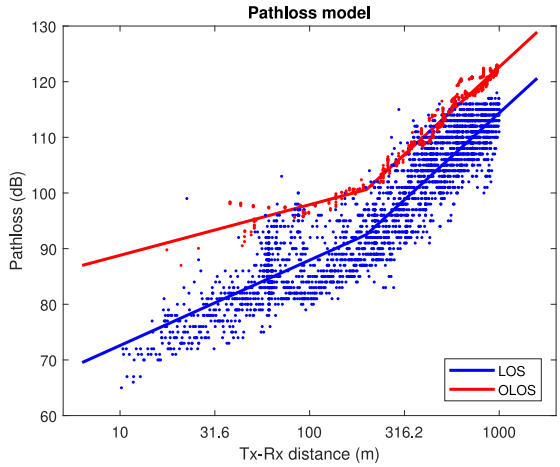

Fig. 2. Dual-slope path-loss model for LOS and OLOS. (The blue and red dots representing the measurement results for LOS and obstructed LOS (OLOS) scenarios).

calculated as

$$d_c = \frac{4h_{Tx}h_{Rx}}{\lambda}, \tag{3}$$

where h_{Tx}, h_{Rx} are the height of the Tx and Rx antennas and λ is the wavelength. If we assume that both, the transmitter and receiver are regular cars, the antenna heights are $h_{Tx} = h_{Rx} =$ 1.5 m, the wavelength is $\lambda = 0.0509$ m at 5.89 GHz and the breaking point distance is $d_c = 176.7$ m.

In order to evaluate the impact of big vehicle shadowing on car-to-car communication, we first carried out measurements of the path-loss in the following two scenarios:

- Car-to-car communication with LOS channel condition.
- Car-to-car communication with LOS blocked by a big bus in between.

For both scenarios, the transmit and receive antennas are placed on top of the cars with height 1.5 m. The distance between the two cars varies from 10 m to 1000 m calculated based on logged GPS locations. The transmitter car is equipped with an on-board-unit (OBU) that transmits the 10 MHz bandwidth DSRC signal at frequency 5.89 GHz. At the receiver car, the received power is continuously logged by a spectrum analyzer. In the second scenario, we arrange a tourist bus to drive in front of the receiver car to block the LOS between the transmitter and receiver cars. The gap between the receiver car and the bus is about 5 m. The bus is 12 m length, 3.5 m height and 2.5 m width.

The measured path-loss versus the distance between the transmitter and receiver is shown inFig. 2. We built a dual-slope path-loss model from the measured data using linear regression. Specifically, the model for LOS is

$$PL_{\text{LOS}}(d) = \begin{cases} 57.2617 + 10 \times 1.5334 \log_{10} d + X_{\sigma_1} & d \le 176.7\text{m} \\ 20.7653 + 10 \times 3.1202 \log_{10} d + X_{\sigma_2} & d > 176.7\text{m} \end{cases}, \tag{4}$$

where X_{σ_1} and X_{σ_2} are zero mean Gaussian random variables with $\sigma_1 = 4.39$ dB and $\sigma_2 = 4.23$ dB. The coefficient of determination R^2 of the linear regression for the dual-slope path-loss model are 0.6601 and 0.9217, respectively. The high value of R^2, especially of the steeper slope, shows the goodness of fit of the predicted model.

The model for OLOS is

$$PL_{\text{OLOS}}(d) = \begin{cases} 79.7089 + 10 \times 0.90925 \log_{10} d + X_{\sigma_1} & d \le 176.7\text{m} \\ 28.3188 + 10 \times 3.1436 \log_{10} d + X_{\sigma_2} & d > 176.7\text{m} \end{cases}, \tag{5}$$

where X_{σ_1} and X_{σ_2} are zero mean Gaussian random variable with $\sigma_1 = 1.74$ dB and $\sigma_2 = 1.24$ dB. In this case, the coefficient of determination R^2 are 0.616 and 0.9579, respectively.

As observed from Fig. 2. The difference between the expected path-loss of LOS and OLOS reaches 17 dB when the transmitter-receiver distance is less than $d_c = 176.7$ m and reduces from 17 dB to 9 dB when this distance is from d_c to 1000 m. The difference between the path-loss in these two models is caused by bus shadowing, and hence is referred to as shadowing loss for one big vehicle in this paper.

In reality, the V2V communication can see multiple big vehicle obstruction. The transmitted signal may experience very complex reflection and diffraction which cause the obstruction loss. According to [33], the research onto the radio wave transmission obstruction has a long history. Some methods to calculate the complex terrain obstruction loss named knife-edge obstruction are popular due to their simplicity. Bullington in [34] considers the loss of knife-edge obstacle by determining the height and the position of the obstacle. Multiple knife-edge obstacles problem is considered by Epstein and Peterson in [35] and Deygout in [36], [37]. The ITU recommendation P.526 incorporates of both the Deygout and Epstein-Peterson methods in [38]. In this recommendation, the individual contribution of each obstacle shadowing loss is added to the total path-loss and the correction term is introduced to have a better approximation in real situation. The correction term can be either positive or negative. In this paper, we have determined the shadowing loss of each big vehicle obstruction by measurement and the shadowing loss of multiple obstacles is the contribution from each of them. Here, we will investigate how this shadowing loss affects the

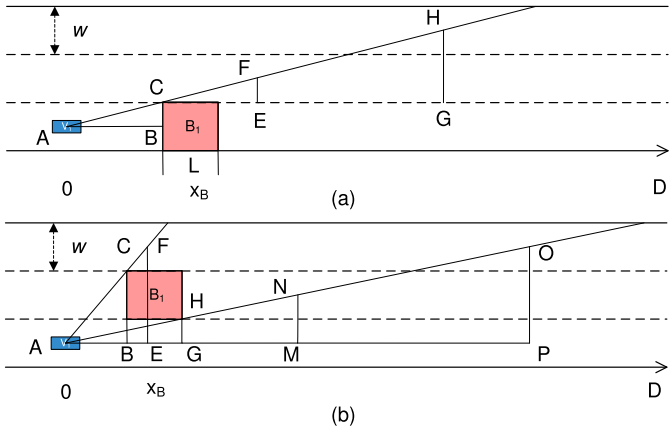

Fig. 3. Mutiple lane road.

packet delivery ratio (PDR) in car-to-car communication in a multi-lane road.

B. Geometrical Shadowing Region

If there is a big vehicle travelling on the road, it may create a shadowing loss for the other vehicles on the road. To investigate the impact of big vehicle shadowing, we first need to find out which regions on the road fall into the shadowing of the bus. The shadow region depends on the relative position of an ordinary vehicle to a big vehicle and the geometrical relation of each pair of ordinary vehicles.

The bus can cause shadowing for two cars on the same lane or an adjacent lane. Here we analyze two cases: i) the bus is on the same lane with the transmitting car as shown in Fig. 3 (a); ii) the bus is on the next lane of the transmitting car as shown in Fig. 3 (b). By symmetry, these two cases will cover all relative positions of the transmitting car, the receiving car and the bus when shadowing takes place.

1) Bus on the Same Lane: For simplicity, we treat the car as a dimensionless point located at the center of the road. The bus's length and width are L and w where the width is equal to the lane road width w. Consider the bus located at position x_B on lane one. Then, all the cars on lane one within the range $x_B + L/2$ to D will suffer from the shadowing loss caused by this bus. As illustrated in Fig. 3(a), the shadowing region on lane two is from position of point E to D. Two triangles, ABC and CEF are equal, and hence the position of E is $2\text{AB} = 2(x_B - L/2) = 2x_B - L$. Furthermore, the shadowing region on lane three is from the position at point G to D. Considering the two triangles ABC and CGH, we have

$$\frac{\text{AB}}{\text{CG}} = \frac{\text{BC}}{\text{GH}} = \frac{\frac{w}{2}}{\frac{3w}{2}} = \frac{1}{3}$$

$$\Rightarrow \quad \text{CG} = 3\text{AB}$$

$$\Rightarrow \quad \text{AG} = 4\text{AB} = 4(x_B - L/2) = 4x_B - 2L.$$

2) Bus on Adjacent Lane: As illustrated in Fig. 3(b), when the bus is on the adjacent lane of the target car, there is no shadowing for the first lane. On the second lane the shadowing region is from point G to point M. Considering the triangle AMN, we have

$$\frac{\text{AG}}{\text{AM}} = \frac{\text{GH}}{\text{MN}} = \frac{\frac{w}{2}}{w} = \frac{1}{2}$$

$$\Rightarrow \quad \text{AM} = 2\text{AG} = 2(x_B + L/2) = 2x_B + L.$$

Therefore, the shadowing region on lane two is from $(x_B + L/2)$ to $(2x_B + L)$. On the third lane the shadowing region is from point F to point O. Considering the triangle AEF, we have

$$\frac{\text{BC}}{\text{EF}} = \frac{\text{AB}}{\text{AE}} = \frac{\frac{3w}{2}}{2w} = \frac{3}{4}$$

$$\Rightarrow \quad \text{AE} = \frac{4\text{AB}}{3} = \frac{4(x_B - L/2)}{3} = \frac{4x_B}{3} - \frac{2L}{3}.$$

Considering the triangle APO, we have

$$\frac{\text{AG}}{\text{AP}} = \frac{\text{GH}}{\text{PO}} = \frac{\frac{w}{2}}{2w} = \frac{1}{4}$$

$$\Rightarrow \quad \text{AP} = 4\text{AG} = 4(x_B + L/2) = 4x_B + 2L.$$

Hence, the shadowing region on lane three is from $(4x_B/3 - 2L/3)$ to $(4x_B + 2L)$.

III. A Stochastic Geometric Approach for Analyzing the Effect of Bus Shadowing

To find the expected shadow region on each lane and the resulting link quality of V2V communication, we need to consider the distribution of cars and buses on each lane. In this section, we first introduce a practical model for vehicle distribution, namely the *hardcore repulsive PPP*, which captures both the randomness of vehicle distribution and the minimum separation between two adjacent vehicles. Then, based on the proposed model, we derive the expected shadowing region and the degradation of the V2V communication quality, caused by buses running on the same lane and the next lane with the tagged vehicle, respectively.

A. Hardcore Repulsive PPP for Vehicle Distribution

On a real road, cars and buses (or trucks) are at random locations and with different density. In many existing works [9]–[11], the vehicles on the road are modeled by a PPP for simplicity. However, this model is too simplistic and ignores the size of the vehicles and their separation requirement for road safety purposes. To this end, we propose a hardcore repulsive PPP, where the distance between adjacent vehicles on the same lane follows a truncated exponential distribution, as follows:

$$f_{\mathbf{d}}(x) \triangleq \Pr(\mathbf{d} = x) = \begin{cases} \lambda e^{-\lambda(x-s)} & x \geq s \\ 0 & \text{otherwise} \end{cases}. \tag{6}$$

This distribution has mean and variance given by

$$\mathbb{E}[\mathbf{d}] = \frac{\lambda s + 1}{\lambda},$$

$$\mathbb{V}\mathrm{ar}[\mathbf{d}] = \mathbb{E}[(\mathbf{d} - \mathbb{E}[\mathbf{d}])^2] = \frac{1}{\lambda^2}.$$

With the distance between two adjacent vehicles modeled by the truncated exponential distribution in (6), the location of the

first[3] n vehicles on a typical road can be represented by

$$V_1 = X_1$$
$$V_2 = X_1 + X_2 + s,$$
$$\cdots$$
$$V_n = \sum_{i=1}^{n} X_i + (n-1)s, \tag{7}$$

where $X_1, X_2, \ldots, X_m$ are exponentially, independently and identically distributed (i.i.d.) random variables with probability density function (p.d.f.): $f(X_i = x) = \lambda e^{-\lambda x}$.

With the proposed hardcore repulsive PPP model as described in (6) and (7), the effective density of the vehicles traveling on a straight road is a function of the parameter λ and the safety distance s as

$$\lambda_e = \frac{1}{\mathbb{E}[\mathbf{d}]} = \frac{\lambda}{\lambda s + 1}. \tag{8}$$

Next, we derive the vehicle distributions based on the adopted distance distribution model in (6). Let $\mathbb{Pr}(n, R)$ be the probability for having n vehicles within the range from the origin to R meters, where $n = 0, 1, ..., \lfloor \frac{R}{s} \rfloor + 1$. Note that deriving $\mathbb{Pr}(n, R)$ directly from the distribution distribution $f_{\mathbf{d}}(x)$ is challenging. Due to the *memoryless* nature of the exponential distribution, the vehicles with distance distribution given in (6) can be generated by the following procedure

- First, we generate the points via the conventional homogeneous PPP with density λ, which is denoted as Φ_V.
- Then, a safety distance s is inserted between each adjacent pair of points.

Based on the above generating procedure, there will be n points within the range according to the distance distribution in (6) if and only if

- There are n points generated by Φ_V within the range $[0, (R-(n-1)s)]$, and
- The $(n+1)$th points generated by Φ_V is beyond the position $(R - nS)$.

Note that the first condition ensures that there will be at least n points within the range $[0, R]$ after inserting the safety distance between each adjacent pair of vehicles, and the second condition ensures that the $(n+1)$th is beyond the range after inserting the safety distance. Above conditions can be equivalently interpreted as

- There are x points generated by Φ_V within the range $[0, R - ns]$ and $x \leq n$;
- There are y points generated by Φ_V within the range $(R - ns, R - ns + s]$ and $x + y \geq n$.

Hence the probability of having n points within range R is given by

$$\mathbb{Pr}(n, R) = \sum_{x=0}^{n} \frac{(\lambda\,(R-ns))^x}{x!} e^{-\lambda(R-ns)} \sum_{y=n-x}^{\infty} \frac{(\lambda s)^y}{y!} e^{-\lambda s}$$
$$= e^{-\lambda(R-ns)} \sum_{x=0}^{n} \frac{(\lambda(R-ns))^x}{x!} \sum_{y=n-x}^{\infty} \frac{(\lambda s)^y}{y!} e^{-\lambda s}$$
$$= e^{-\lambda(R-ns)} \sum_{x=0}^{n} \frac{(\lambda(R-ns))^x}{x!} \left(1 - e^{-\lambda s} \sum_{y=0}^{n-x-1} \frac{(\lambda s)^y}{y!}\right)$$
$$= e^{-\lambda(R-ns)} \sum_{x=0}^{n} \frac{(\lambda(R-ns))^x}{x!} \left(1 - \frac{\Gamma(n-x, \lambda s)}{(n-x)!}\right)$$
$$= e^{-\lambda(R-ns)} \left(\frac{(\lambda(R-ns))^n}{n!} + \sum_{x=0}^{n-1} \frac{(\lambda(R-ns))^x}{x!(n-x-1)!} \gamma(n-x, \lambda s)\right), \tag{9}$$

where $\gamma(a, x)$ and $\Gamma(a, x)$ are the incomplete gamma function lower and upper part defined by $\gamma(a, x) = \int_0^x e^{-t} t^{a-1} dt$ and $\Gamma(a, x) = \int_x^\infty e^{-t} t^{a-1} dt$. For $n = \lfloor R/s \rfloor + 1$ we can use

$$\mathbb{Pr}(\lfloor R/s \rfloor + 1, R) = 1 - \sum_{n=0}^{\lfloor R/s \rfloor} \mathbb{Pr}(n, R). \tag{10}$$

Based on the proposed hardcore repulsive PPP model, we will investigate the effect of big vehicle shadowing on the PDR of car-to-car communication in the following subsections.

B. Shadow Region and Broken Links

In this section, we analyze the expected shadow region and the number of cars that have broken links with the tagged car due to the bus shadowing. We consider the following two scenarios.

1) Bus in the Same Lane as the Target Vehicle: We assume that the tagged car is on lane one at position 0 and the vehicle locations follow a hardcore repulsive PPP as discussed in the previous subsection. Note that a typical vehicle on lane one can either be a car or a bus/truck, which may cause obstruction of the signal. We define P_B as the probability that a random vehicle is identified as a bus, hence $1 - P_B$ is the probability that this vehicle is a car.

We further denote by x_B the horizontal location of the bus and x_{ci} the position of a car on lane i, where $i = 1, 2, 3$. Conditioned on the existence of the target vehicle on lane one at the origin, the first vehicle appears only at the location s and beyond, which implies that $x_B \geq s$. Beyond the safety distance s, the distribution of the remaining vehicles can be modeled by the hardcore repulsive PPP.

Following the analysis in Section II.B, from target vehicle on lane one the geometrical shadow region caused by bus at x_B on lane one is from $(x_B + L/2)$ to D, on lane two is from $(2x_B - L)$ to D and on lane three is from $(4x_B - 2L)$ to D respectively.

We can now compute the probability that a location is not in the shadowing region of any bus. The location x_{C1} is not shadowed if there is no bus in the region $(0, x_{C1} - L/2)$. However, we already know that there is no vehicle within $[0, s]$, hence we only need to consider the region $(s, D]$. The probability that location x_{C1}, for $x_{C1} \in (s, D]$, is not in the shadowing region is equivalent to

- There is no vehicle within the range with probability $\mathbb{Pr}(s, x_{C1} - L/2)$, or
- There are k vehicles within the range, but they are not buses.

[3]The origin is marked as the end of the road or a turn of the road.

This probability can be computed by

$$P_{SD}(x_{c1}) = \sum_{k=0}^{\infty}(1-P_B)^k \mathbb{P}\mathbb{r}\left(k, x_{c1} - \frac{L}{2} - s\right), \quad (11)$$

where $\mathbb{P}\mathbb{r}(n,R)$ is the probability for having n vehicles within range R in the hardcore repulsive PPP model. Then, the expected length of the shadow region on lane one can be derived as

$$\begin{aligned}\overline{SD_{11}} &= \int_s^D \left(1-\sum_{k=0}^{\infty}(1-P_B)^k \mathbb{P}\mathbb{r}\left(k, x_{c1}-\frac{L}{2}-s\right)\right) dx_{c1} \\ &= (D-s)-\sum_{k=0}^{\infty}(1-P_B)^k \int_s^D \mathbb{P}\mathbb{r}\left(k, x_{c1}-\frac{L}{2}-s\right) dx_{c1}.\end{aligned} \quad (12)$$

Similarly, the shadow region on lane two and three are

$$\begin{aligned}\overline{SD_{12}} = {} & (D-(2s-L)) - \\ & -\sum_{k=0}^{\infty}(1-P_B)^k \int_{2s-L}^D \mathbb{P}\mathbb{r}\left(k, \frac{x_{c2}+L}{2} - s\right) dx_{c2},\end{aligned} \quad (13)$$

$$\begin{aligned}\overline{SD_{13}} = {} & (D-(4s-L)) - \\ & -\sum_{k=0}^{\infty}(1-P_B)^k \int_{4s-L}^D \mathbb{P}\mathbb{r}\left(k, \frac{x_{c3}+2L}{4} - s\right) dx_{c3},\end{aligned} \quad (14)$$

respectively.

Next, we derive the expected number of cars that cannot successfully receive the packet from the target vehicle due to bus shadowing. The communication link between a typical car and the target vehicle suffers from both path-loss and possibly the shadow loss caused by a bus. We define the shadow loss caused by a single bus as P_{SL}, which is obtained from our measurement results as the difference between received power in LOS and OLOS scenarios.[4] If a vehicle falls into the overlapping shadow region of m buses the shadow loss is mP_{SL}. Based on this channel model, we can obtain the maximum communication range from the target vehicle to another car on lane i, under the shadowing of m buses, which is denoted by $d^{(i)}_{\max}(m)$. This distance can be calculated as

$$d^{(i)}_{\max}(m) = \left(\frac{P_T}{m \cdot P_0 \cdot P_{SL} \cdot P_{th}}\right)^{\frac{1}{\alpha}}, \quad (15)$$

where P_T is the transmit power, P_0 is reference power in path-loss model, P_{th} is the threshold power (or sensitivity) of the receiver, α is the attenuation factor of path-loss model. We further denote $\hat{m}(x_{Ci})$ as the maximum number of bus shadowing which allows a car at location x_{Ci} to admit a connection

$$\hat{m}(x_{Ci}) = \arg\max_m \left[x_{Ci} < d^{(i)}_{\max}(m)\right].$$

[4]Recall that based on our measurement, the shadowing loss range between 9 dB to 17 dB, depending on the separation between the transmitting and receiving vehicles. However, it is difficult to obtain the exact model for the shadowing loss. For ease of analysis, we have approximate it by the expected value. Note that the shadowing loss, considered in our paper, agrees with other previous measurements in [10] and [11] where the loss is from 8.6 dB to 20 dB.

On lane one, a car at x_{C1} can communicate with the target vehicle at the origin if no more than $\hat{m}(x_{C1})$ buses are within the range $[s, x_{C1}-s]$. Therefore, the probability that a car at x_{C1} can successfully receive the information from the target vehicle is

$$\begin{aligned}Pb_{11}(x_{C1}) = {} & \sum_{v=0}^{\hat{m}(x_{C1})} \mathbb{P}\mathbb{r}(v, x_{C1}-2s) + \\ & + \sum_{v=\hat{m}(x_{C1})+1}^{\infty} \sum_{b=0}^{\hat{m}(x_{C1})} \binom{v}{b} P_B^b (1-P_B)^{v-b} \mathbb{P}\mathbb{r}(v, x_{C1}-2s),\end{aligned} \quad (16)$$

where the first sum corresponds to the probability that there are no more than $\hat{m}(x_{C1})$ *vehicles* and the second sum corresponds to the case that there are more than $\hat{m}(x_{C1})$ *vehicles* but less than $\hat{m}(x_{C1})$ *buses*. On lane one, beyond s, the distribution of the vehicle is independent of the exact location. Therefore, the probability that there is a vehicle at a typical location x_{C1} is λ_e, which is the effective density of vehicles defined in (8). Furthermore, a vehicle is identified as a bus with probability P_B and a car with probability $1-P_B$. Hence, the probability there is a car at location x_{C1} on lane one is given by

$$P_{car}(x_{Ci}) = \begin{cases} 0, & x_{Ci} < s \\ (1-P_B)\lambda_e, & x_{Ci} \geq s \end{cases}.$$

On lane two and lane three, there are no buses. Hence, the probability that there is a car at location x_{C2} and x_{C3} is given by λ_e. The expected number of cars on lane one within the communication range is

$$N_{11} = \int_s^D Pb_{11}(x_{C1})(1-P_B)\lambda_e dx_{C1}. \quad (17)$$

Similarly, the expected number of cars on lane two and three that can successfully receive the packets sent by the target vehicle is

$$N_{1i} = \int_0^D Pb_{1i}(x_{Ci})\lambda_e dx_{Ci}, \quad i = 2, 3, \quad (18)$$

where

$$\begin{aligned}Pb_{12}(x_{C2}) = {} & \sum_{v=0}^{\hat{m}(x_{C2})} \mathbb{P}\mathbb{r}\left(v, \frac{x_{C2}+L}{2} - s\right) + \\ & + \sum_{v=\hat{m}(x_{C2})+1}^{\infty} \sum_{b=0}^{\hat{m}(x_{C2})} \binom{v}{b} P_B^b (1-P_B)^{v-b} \mathbb{P}\mathbb{r}\left(v, \frac{x_{C2}+L}{2} - s\right),\end{aligned} \quad (19)$$

and

$$\begin{aligned}Pb_{13}(x_{C3}) = {} & \sum_{v=0}^{\hat{m}(x_{C3})} \mathbb{P}\mathbb{r}\left(v, \frac{x_{C3}+2L}{4} - s\right) + \\ & + \sum_{v=\hat{m}(x_{C3})+1}^{\infty} \sum_{b=0}^{\hat{m}(x_{C3})} \binom{v}{b} P_B^b (1-P_B)^{v-b} \mathbb{P}\mathbb{r}\left(v, \frac{x_{C3}+2L}{4} - s\right).\end{aligned} \quad (20)$$

We also can estimate the total number of vehicle on each lane as

$$N_{11}^T = (1 - P_B)\lambda_e(D - s), \tag{21}$$

$$N_{12}^T = \lambda_e \left(D - \frac{1}{2}\left(s - \frac{1}{\lambda} \right) \right), \tag{22}$$

$$N_{13}^T = \lambda_e \left(D - \frac{1}{2}\left(s - \frac{1}{\lambda} \right) \right). \tag{23}$$

The difference between the total number of cars and the number of cars within communication range is the expected number of cars that fail to receive the packets from the target vehicle due to the shadowing loss caused by the buses on lane one.

2) Bus in the Adjacent Lane to the Target Vehicle: In this case, the car on lane one is not shadowed by a bus, we will analyze the shadow effect for cars on lane two and three.

Since the vehicles in different lanes are independently distributed, the origin marked by the target vehicle can be in any place between two cars on the next lane. Assuming that vehicles in the adjacent lane to the target vehicle are at $V_1^2, V_2^2, \ldots, V_n^2$, we can write

$$V_1^2 = U(X_1 + s), \tag{24}$$

where U is a uniformly distributed random variable within range [0,1]. The next vehicle can be obtained by

$$V_2^2 = V_1^2 + X_2 + s,$$

$$\cdots$$

$$V_n^2 = V_1^2 + \sum_{i=2}^{n} X_i + (n-1)s.$$

Note that V_1^2 includes the product of two random variables, e.g. the uniformly distributed random variable (r.v.) U and the exponentially distributed r.v. X_1. It is challenging to obtain the closed-form expression for the distribution of V_1^2. For simplicity, we approximate it by an shifted exponential r.v., which maintains the same expected value. Specifically, we approximate V_1^2 as:

$$V_1^2 \approx X_1 + \frac{1}{2}\left(s - \frac{1}{\lambda} \right) = X_1 + \Delta,$$

where $\Delta = 1/2(s - 1/\lambda)$ is the offset we add to ensure the same expected value as the original V_1^2 defined in Eq. (24). The main motivation for the above approximation is to apply the analytical results derived for the hardcore repulsive PPP directly. Then, we have

$$V_n^2 = \sum_{i=1}^{n} X_i + (n-1)s + \Delta,$$

where the first two parts are same as the result we derived in the previous section.

From the geometrical shadowing analysis we know the shadow region on lane two is from $x_B + L/2$ to $2x_B + L$. The probability that there is no shadowing at x_{C2} is equivalent to no bus within the range $[(x_{C2} - L)/2, x_{C2} - L/2]$ with its length $x_{C2}/2$. Hence the expected shadow region length on lane two is

$$\overline{SD_{22}} = \int_0^D \left(1 - \sum_{k=0}^{\infty} (1 - P_B)^k \mathbb{P}\mathbb{r}\left(k, \frac{x_{c2}}{2} - \Delta \right) \right) dx_{c2}. \tag{25}$$

Similarly, the expected shadow region length on lane three is

$$\overline{SD_{23}} = \int_0^D \left(1 - \sum_{k=0}^{\infty} (1 - P_B)^k \mathbb{P}\mathbb{r}\left(k, \frac{x_{c3} + 2L}{2} - \Delta \right) \right) dx_{c3}. \tag{26}$$

Because there is no shadowing on lane one, the target vehicle can communicate with all vehicles in lane one. The expected number of cars in lane one is

$$N_{21} = \lambda_e(D - s). \tag{27}$$

in lane two, a car at x_{c2} can communicate with the target vehicle at the origin if no more than $m(x_{c2})$ buses are within the range $[(x_{C2} - L)/2, x_{C2} - L/2]$. Conditioned on the existence of a vehicle at x_{C2}, there is no vehicle within $[x_{C2} - s, x_{C2}]$ due to the safety distance. Then, the range of interest is $[(x_{C2} - L)/2, x_{C2} - s]$ with length $[x_{C2}/2 - s + L/2]$. The probability that a car is within communication range is

$$Pb_{22}(x_{C2}) = \sum_{v=0}^{\hat{m}(x_{C2})} \mathbb{P}\mathbb{r}\left(v, \frac{x_{C2} + L}{2} - s - \Delta \right) + \\ + \sum_{v=\hat{m}(x_{C2})+1}^{\infty} \sum_{b=0}^{\hat{m}(x_{C2})} \binom{v}{b} P_B^b (1 - P_B)^{v-b} \\ \times \mathbb{P}\mathbb{r}\left(v, \frac{x_{C2} + L}{2} - s - \Delta \right). \tag{28}$$

The expected number of cars in lane two within communication range is

$$N_{22} = \int_0^D Pb_{22}(x_{C2})(1 - P_B)\lambda_e dx_{C2}. \tag{29}$$

We have a similar result for the number of cars in lane three

$$N_{23} = \int_0^D Pb_{23}(x_{C3})(1 - P_B)\lambda_e dx_{C3}, \tag{30}$$

where

$$Pb_{23}(x_{C3}) = \sum_{v=0}^{\hat{m}(x_{C3})} \mathbb{P}\mathbb{r}\left(v, \frac{x_{C3} + 2L}{2} - s - \Delta \right) + \\ + \sum_{v=\hat{m}(x_{C3})+1}^{\infty} \sum_{b=0}^{\hat{m}(x_{C3})} \binom{v}{b} P_B^b (1 - P_B)^{v-b} \\ \times \mathbb{P}\mathbb{r}\left(v, \frac{x_{C3} + 2L}{2} - s - \Delta \right). \tag{31}$$

The total number of vehicles in each lane is

$$N_{21}^T = \lambda_e(D - s), \tag{32}$$

$$N_{22}^T = (1 - P_B)\lambda_e(D - \Delta), \tag{33}$$

$$N_{23}^T = (1 - P_B)\lambda_e(D - \Delta). \tag{34}$$

These values are used to calculate the number of broken links to the target vehicle.

IV. Packet Collision Analysis

In the previous section, we have analysed the expected number of cars that have broken links with the target vehicle due to bus shadowing. In practice, even for the established links, the receivers may still fail to receive the packet due to collisions. The packet collision probability mainly depends on the number of interfering cars (whose transmission can cause packet collision at the receiver car) for a given transmitter-receiver pair. In this section, we analyse the impact of bus shadowing on the packet collision probability.

We categorize the interfering cars into two types, namely visible cars and hidden cars. Visible cars can sense the transmission from the target vehicle, while hidden cars can not sense the transmission from the target vehicle. Due to the presence of big vehicles, the number of interfering cars depends on the position of the target vehicle, receiver car and bus lane. Let us assume that the target vehicle T_x is in lane m, the receiver car R_x is in lane n and buses are in lane k. For this scenario, let $\mathcal{V}_{t|mnk}$ and $\mathcal{H}_{t|mnk}$ be the total number of visible and hidden cars, respectively. Calculation of $\mathcal{V}_{t|mnk}$ and $\mathcal{H}_{t|mnk}$ is shown in the latter part of this section. The average packet collision probability for the above scenario can be written as

$$\tau_{mnk} = 1 - (1 - \tau_{s|mnk})(1 - \tau_{h|mnk}) \tag{35}$$

where $\tau_{s|mnk}$ is the collision probability due to the visible interfering cars and $\tau_{h|mnk}$ is the collision probability due to the hidden interfering cars. For the sake of convenience, we drop the subscript mnk in the rest of the analysis. Following the collision probability analysis of [1], [39], τ_s can be written as

$$\tau_s = p_{sc} \times p_b \tag{36}$$

where p_{sc} is the probability that at least one visible car selects a given slot to start its transmission and p_b is the probability to sense the channel busy when a packet is generated. Furthermore, p_{sc} can be expressed as

$$p_{sc} = 1 - (1 - \bar{t}_q p_s)^{\mathcal{V}_t} \tag{37}$$

where $\bar{t}_q$ is the average time the queue is not empty, and p_s is the probability that an sensing vehicle attempts to transmit in an arbitrary slot while it has a packet to transmit. Considering that a random counter between 0 and W is chosen for the backoff procedure, p_s can be approximated as

$$p_s = \frac{1}{W+1} \tag{38}$$

In in (37), $\bar{t}_q$ is derived as

$$\bar{t}_q = f_b(\bar{t}_a + t_{is} + t_T) \tag{39}$$

where $\bar{t}_a$ is the average access time, t_{is} is the initial interframe space, f_b is the packet generation rate at each car, and t_T is the average duration of a transmission. Since all messages are assumed of the same size, the duration of a transmission t_T is a constant, which, following the IEEE 802.11p specifications, can be approximated as

$$t_T = 8\frac{B_b}{R} + t_{ov} \tag{40}$$

where B_b is the packet size, R is the raw data rate and t_{ov} is the PHY overhead. Since the access time is equal to the average backoff time $\bar{t}_{bo}$ when the channel is sensed busy, and null otherwise, $\bar{t}_a$ is given by

$$\bar{t}_a = p_b \bar{t}_{bo}, \tag{41}$$

where the average backoff time $\bar{t}_{bo}$ is equal to

$$\bar{t}_{bo} = [t_s(1 - p_{sc}) + (t_s + t_{is} + t_T)p_{sc}]\frac{W}{2}, \tag{42}$$

where t_s is slot duration. We calculate p_b as

$$p_b = \frac{t_{is} + t_T}{T_b}(1 - \tau_s/2)(1 - \mathcal{V}_t). \tag{43}$$

On the other hand, the collision probability due to the hidden vehicles is given by,

$$\tau_h = 1 - \exp\left(-f_b \mathcal{H}_t t_T\right) \times \left(1 - \frac{t_{is} + t_T}{T_b}(1 - \tau_s/2)\mathcal{H}_t)\right), \tag{44}$$

where the term $\exp(-f_b \mathcal{H}_t t_T)$ represents the probability that no hidden vehicle starts its transmission during the transmission of the target vehicle with the remainder of the equation representing the probability that no hidden terminal is transmitting at a given instant.

In the following, we present the procedure to calculate the total number of visible and hidden cars for a given scenario. The total number of visible and hidden cars can be calculated from $\mathcal{V}_{t|mnk} = \sum_{i=1}^{3} \mathcal{V}_{i|mnk}$ and $\mathcal{H}_{t|mnk} = \sum_{i=1}^{3} \mathcal{H}_{i|mnk}$, where $\mathcal{V}_{i|mnk}$ and $\mathcal{H}_{i|mnk}$ are the average number of visible and hidden cars, respectively, in lane $i \in \{1, 2, 3\}$. For the sake of simplicity, we assume that the strength of an interfering signal needs to be more than the carrier sensing threshold P_{cs} to cause a packet collision at the receiver. With this assumption, we have the equations for $\mathcal{V}_{i|mnk}$ and $\mathcal{H}_{i|mnk}$ (45) and (46), shown at the bottom of this page.

$$\mathcal{V}_{i|mnk} = \frac{\int_{x_{R_x}} \Pr(x_{R_x}, P_{th}, mnk) \int_{x_{I_x}} \Pr(|x_{I_x}|, P_{cs}, mik) \Pr(|x_{I_x} - x_{R_x}|, P_{cs}, ink) \lambda_e dx_{I_x} dx_{R_x}}{\int_{x_{R_x}} \Pr(x_{R_x}, P_{th}, mnk) dx_{R_x}} \tag{45}$$

$$\mathcal{H}_{i|mnk} = \frac{\int_{x_{R_x}} \Pr(x_{R_x}, P_{th}, mnk) \int_{x_{I_x}} (1 - \Pr(|x_{I_x}|, P_{cs}, mik)) \Pr(|x_{I_x} - x_{R_x}|, P_{cs}, ink) \lambda_e dx_{I_x} dx_{R_x}}{\int_{x_{R_x}} \Pr(x_{R_x}, P_{th}, mnk) dx_{R_x}} \tag{46}$$

In (45) and (46), $\Pr(x, P, mnk)$ is the probability that the received signal strength is larger than P with transmitter-receiver distance of x provided that transmitter in lane m, receiver in lane n and buses in lane k. This probability can be calculated from the analysis shown in the earlier section. For example, with the target vehicle in lane 2, the receiver car in lane 1 and buses in lane 2, the average number of visible cars from lane 3 is shown in eq. (47), shown at the bottom of this page. Following equations (19) and (31), $\Pr(x_{R_x}, P_{th}, 212)$, $\Pr(|x_{I_x}|, P_{cs}, 232)$, $\Pr(|x_{I_x} - x_{R_x}|, P_{cs}, 312)$ in (47) are given by

$$\Pr(x_{R_x}, P_{th}, 212) = \sum_{v=0}^{\hat{m}(x_{R_x})} \mathbb{P}\mathbb{r}\left(v, \frac{x_{R_x}+L}{2} - s\right) + \\ + \sum_{v=\hat{m}(x_{R_x})+1}^{\infty} \sum_{b=0}^{\hat{m}(x_{R_x})} \binom{v}{b} p_B^b (1-p_B)^{v-b} \mathbb{P}\mathbb{r}\left(v, \frac{x_{R_x}+L}{2} - s\right), \tag{48}$$

$$\Pr(|x_{I_x}|, P_{cs}, 232) = \sum_{v=0}^{\overline{m}(|x_{I_x}|)} \mathbb{P}\mathbb{r}\left(v, \frac{|x_{I_x}|+L}{2} - s\right) \\ + \sum_{v=\overline{m}(|x_{I_x}|)+1}^{\infty} \sum_{b=0}^{\overline{m}(|x_{I_x}|)} \binom{v}{b} p_B^b (1-p_B)^{v-b} \\ \times \mathbb{P}\mathbb{r}\left(v, \frac{|x_{I_x}|+L}{2} - s\right), \tag{49}$$

$$\Pr\left(|x_{I_x} - x_{R_x}|, P_{cs}, 312\right) \\ = \sum_{v=0}^{\overline{m}(|x_{I_x}-x_{R_x}|)} \mathbb{P}\mathbb{r}\left(v, \frac{|x_{I_x}-x_{R_x}|+2L}{2} - s - \Delta\right) \\ + \sum_{v=\overline{m}(|x_{I_x}-x_{R_x}|)+1}^{\infty} \sum_{b=0}^{\overline{m}(|x_{I_x}-x_{R_x}|)} \binom{v}{b} p_B^b (1-p_B)^{v-b} \times \\ \mathbb{P}\mathbb{r}\left(v, \frac{|x_{I_x}-x_{R_x}|+2L}{2} - s - \Delta\right). \tag{50}$$

In the above equations, $\overline{m}(x_{Ci})$ is defined by (following the definition of $\hat{m}(x_{Ci})$)

$$\overline{m}(x_{Ci}) = \arg\max_{m} \left[x_{Ci} < \left(\frac{P_T}{P_0 m P_{SL} P_{cs}}\right)^{\frac{1}{\alpha}}\right].$$

V. Simulation Results and Discussion

The simulation model is based on the system architecture described in previous Sections. We have implemented a Matlab based simulator to evaluate the impact of the big vehicle shadowing on V2V communications. Specifically, we consider a section of highway with three lanes, where the vehicles are generated based on the hardcore repulsive PPP model introduced in Section III For the sake of simplicity, the vehicles are assumed to be stationary within the duration of one packet transmission. This is a reasonable assumption as [40] and [11] show that the estimated link breaking probability is very small at a speed of less than 120 miles/hour. In the simulation, each vehicle transmits safety messages in a conventional half-duplex manner with a rate of 10 Hz. The parameters used in the simulation are listed in the Table I.

TABLE I
Simulation Parameters

Parameter	Notation	Value
Bus length	L	12 m
Inter-vehicle spacing (safety distance)	$s = 2L$	24 m
Lane width	w	3 m
Region of interest	$D = x^{\mathrm{L}}_{\max}(3)$	478.3 m
Vehicle density on each lane	λ	50 per km
Probability of a vehicle is a bus	P_B	0.1-0.8
Transmit power	P_{T}	23 dBm
Path-loss at reference point	P_0	[57.2 20.7] dB
Path-loss attenuation	α	[1.53 3.12]
Receiver sensitivity	P_{th}	-75 dBm
Decoding sensitivity		-75 dBm
Carrier sensing sensitivity	P_{cs}	-80 dBm
Packet rate	f_b	10 Hz
Packet size	B_b	200 Bytes
Maximum contention window	W	15
Slot duration	t_s	13 μs
Inter-frame space	t_{is}	58 μs
Physical layer overhead per packet	t_{ov}	40 μs

The bus length and the lane width are chosen based on typical vehicle and road dimensions. Because the safety distance s is calculated from center to center of vehicles, we set this value to two times the length of a bus. The vehicle densities are the same for all three lanes of the road as $\lambda = 0.05$, 50 vehicles per km. The region of interest is the maximum communication range in lane three while there is no bus obstruction, e.g. $D = 478.3$ m[5]. This region is calculated based on the measured path-loss model has been shown in Section II. The probability that a vehicle is a bus varies from 0.1 to 0.8.

In Fig. 5, we plot the expected shadowing region length for the scenario where the bus is in the same lane as the target vehicle. First, it is observed that the analytical results match the simulation results very well. Furthermore, it is observed that the shadow region in lane one is the biggest, it increases from more than 200 m to 430 m when the bus density increases. This trend is similar for the shadow region in lane two and three. However, due to optical perspective the shadow region in lane two and three is smaller than that in lane one. In Fig 6, we plot the expected shadowing region length for the scenario where the bus is in the

[5]Note that the region of interest has impact on the PDR performance as PDR depends on the number of cars in the communication range and the total cars in the region of interest. For a given number of buses on the road, increasing the region of interest will decrease the PDR as the total cars in the region of interest will increase while number of cars in the communication range remains the same.

$$\mathcal{V}_{3|212} = \frac{\int_{x_{R_x}=0}^{D} \Pr(x_{R_x}, P_{th}, 212) \int_{x_{I_x}=x_{R_x}-D_{cs}}^{x_{R_x}+D_{cs}} \Pr(|x_{I_x}|, P_{cs}, 232) \Pr(|x_{I_x} - x_{R_x}|, P_{cs}, 312) \lambda_e dx_{I_x} dx_{R_x}}{\int_{x_{R_x}=0}^{D} \Pr(x_{R_x}, P_{th}, 212) dx_{R_x}} \tag{47}$$

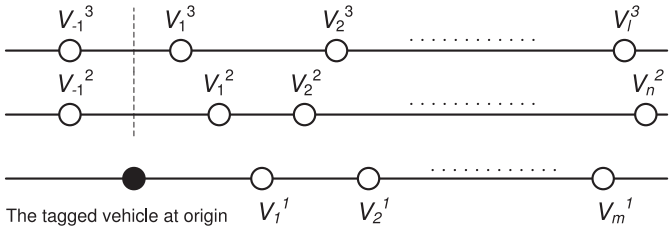

Fig. 4. Hardcore repulsive PPP for multiple-lane road.

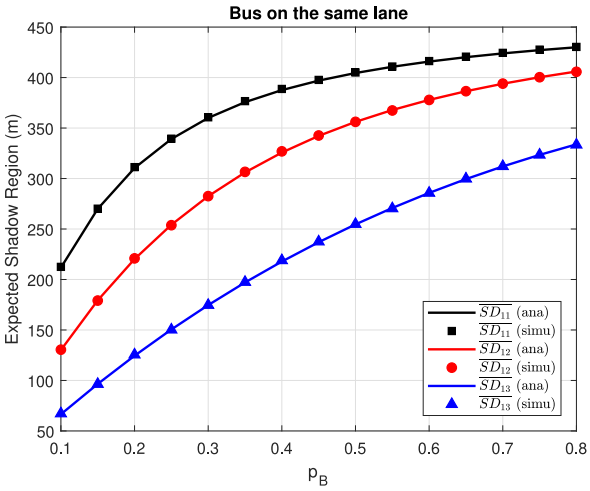

Fig. 5. Expected shadow region length-Bus in the same lane as the target vehicle.

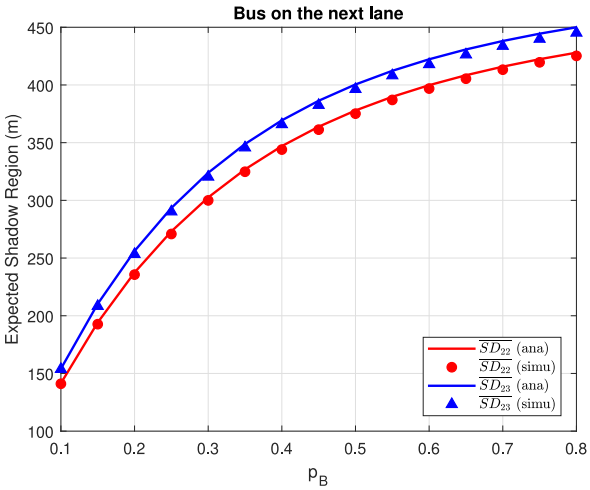

Fig. 6. Expected shadow region length-Bus in the adjacent lane to the target vehicle.

adjacent lane to the target vehicle. It is observed that the shadow region length increases quickly with the increase in probability that a vehicle is a bus. The maximum shadow region can be up to 450m in lane three when most of the vehicles traveling in lane two are buses.

If a car is obstructed by many buses, it cannot communicate with the target vehicle. We define the ratio of the number of cars that can communicate with the target vehicle to the total number of cars for each lane as a link quality metric. This ratio versus

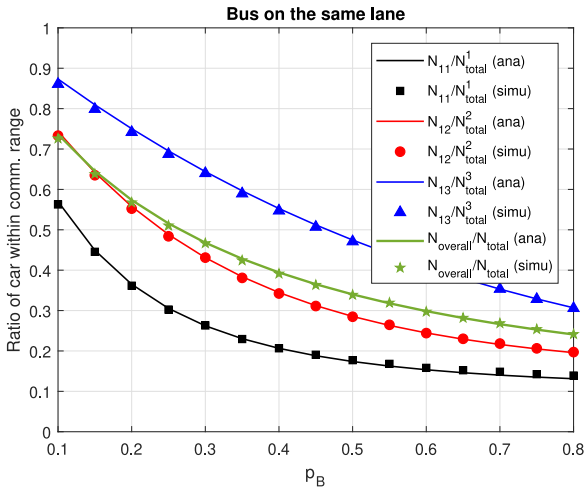

Fig. 7. Car within communication range for the case when the bus is in the same lane as the target vehicle.

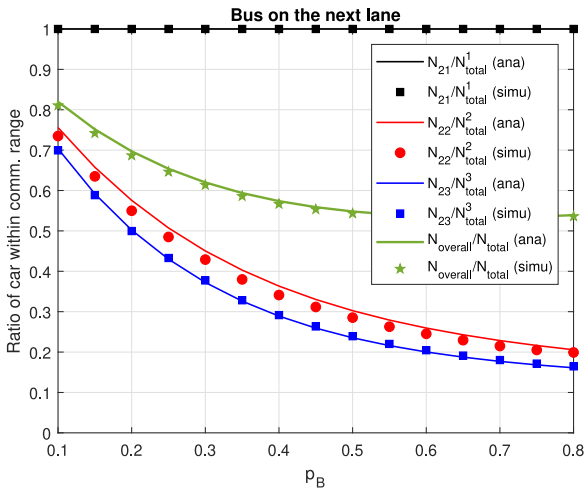

Fig. 8. Car within communication range for the case when the bus is in the adjacent lane to the target vehicle.

the bus density when the bus is in lane one is shown in Fig. 7. When P_B increases from 0.1 to 0.8, the number of cars that can communicate with the target vehicle reduces from more than 70% to only a little more than 20%. A car in lane one suffers the most serious shadowing, as shown in Fig. 5, as it has the lowest number of cars within the communication range of the target vehicle. When the bus is in lane two, the number of cars within the communication range is illustrated in Fig. 8. In this scenario, because the car in lane one is not shadowed by the bus, all of the cars in lane one are within the communication range of the target vehicle and the overall number of cars that can communicate with the targeted vehicle is higher than in the previous scenario. Here, the percentage of cars within the communication range varies from 52% to 80%. We also discuss the impact of vehicle's length and the region of interest. Since the big vehicles may have different length between 6 m to 24 m, we carry out a simulation scenario where the bus's length is randomly and uniformly distributed in the range from 6 m to

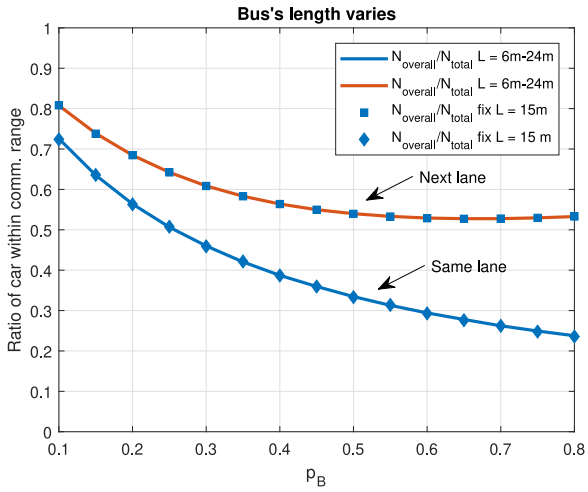

Fig. 9. Car within communication range. Comparison when bus length varies.

24 m. For this scenario, we show the number of cars within the communication range in Fig. 9 and compare the results with fixed bus length scenario ($L = 15$ m). The high agreement between fixed and varied bus's length results in Fig. 9 shows that our model can be applied for different type of the big vehicle.

We present the collision probability results in Fig. 10 while considering buses in lane one. In Fig. 10a, we show the packet collision probability in different lanes provided that the target vehicle T_x is in lane one. The lowest packet collision rate is observed for receiver in the bus lane (i.e., lane one). The rationale behind this phenomenon is as follows. When the receiver is in lane one, the number of hidden nodes is less than in the other cases as the potentially hidden cars' (the cars that cannot sense a transmission from T_x) transmission range is limited to lane one (due to the presence of buses) and hence cannot cause a collision at the receiver. Note that the transmission range of hidden cars drops significantly with the increase in the share of buses and thus, we observe that the collision probability in lane one decays as the proportion of buses increases. On the other hand, for the case with the receiver in lane two or three, there exists a LOS communication link between the receiver and potential hidden cars in lane two or three. In other words, the number of hidden cars is higher when the receiver is in lane two or three rather than when the receiver is in lane one. As a result, a higher packet collision probability is observed for a receiver in lane two or three, compared to a receiver in lane one. For these cases (i.e., receiver in lane two or three), as the proportion of buses increases, the number of hidden cars in lane one decreases while the number of hidden cars in lane two or three increases. Hence, we observe a slight variation in collision probability as the proportion of buses increases. In Fig. 10b and Fig. 10b, we show the packet collision probability in different lanes provided that the vehicle T_x is in lane two or three, respectively. Similar to the results in Fig. 10a, we observe the lowest collision probability for a receiver in lane one due to the limited transmission range of hidden cars. For a receiver in any lane, we observe that the collision probability decreases as the bus proportion increases. This is because the number of interfering cars in lanes two and three is independent of the bus share, while the number of hidden cars in lane one decreases as the bus share increases. Compared to Fig. 10a, we observe a lower collision probability in Fig. 10b and Fig. 10b for any given receiver position. This was expected as the target vehicle in lane two or three gives better transmission range than a target vehicle in lane one and hence the former scenario suffers from less packet collision due to the hidden cars.

Fig. 11 shows the packet delivery ratio (PDR) when a bus is in lane one and the target vehicle is either in lane one, two, or three, respectively. In these three scenarios corresponding to the position of the target vehicle, we present the PDR for each lane and the average PDR for the whole system. In Fig. 11a, the PDR of the target vehicle when it is in lane one is shown. When the bus density increases (P_B increases from 0.1 to 0.8), the PDR reduces from 0.5 to 0.15. The car in lane one suffers the biggest loss of packet transmission because s bus is in lane one. The car in lane three suffers the smallest packet loss. Compared to the results in Fig. 7, we can see a close relationship between the PDR and the number of cars within the communication range of the target vehicle. The results of PDR in Fig. 11 follow the behavior of the results in Fig. 7 and take into account the collision probability. The PDR results when the target vehicle is in lane two and three are shown in Fig. 11b and Fig. 11c. The target vehicle is is a different lane to the bus and the PDRs are much higher than in the previous scenario. In these scenarios, the overall PDRs vary from about 0.8 to 0.65 and 0.82 to 0.7 when the target vehicle is in lane two and three respectively. One special behavior of the PDR is noted in these two scenarios, the PDRs for lane two and three increase when the bus density in lane one increases. This can be explained as follow, when the probability of a vehicle in lane one is a bus P_B increases, the number of cars in lane one decreases which causes a reduction of packet collision for the cars in lane two and three and thus the PDRs of the target vehicles in these lanes slightly increase.

In Fig. 12, we present the collision probability results when the buses are in lane 2. In the first scenario (Fig. 12a), we consider the target vehicle in lane one. For this scenario, the lowest packet collision probability is observed for a receiver in lane two, since the presence of buses reduces the packet collision capability of interfering cars. On the other hand, we observe the highest packet collision probability for receiver at lane 3. Compared to the case with a receiver in lane one, there exist more hidden cars for a receiver in lane three due to the target vehicle's limited transmission range in lane 3 and LOS link between cars in lane 3. As the proportion of buses increases, the transmission range of interfering cars decreases for a receiver in lane one or two and hence, we observe a decrease in packet collision probability for these cases. On the other hand, the packet collision probability for a receiver in lane one does not vary much with increasing proportion of buses. For this case, although the number of interfering cars from lane one and two decreases as the proportion of buses increases, the number of interfering cars in lane three increases. In Fig. 12a, we present the collision probability results for the target vehicle in lane two. Again, we observe the lowest

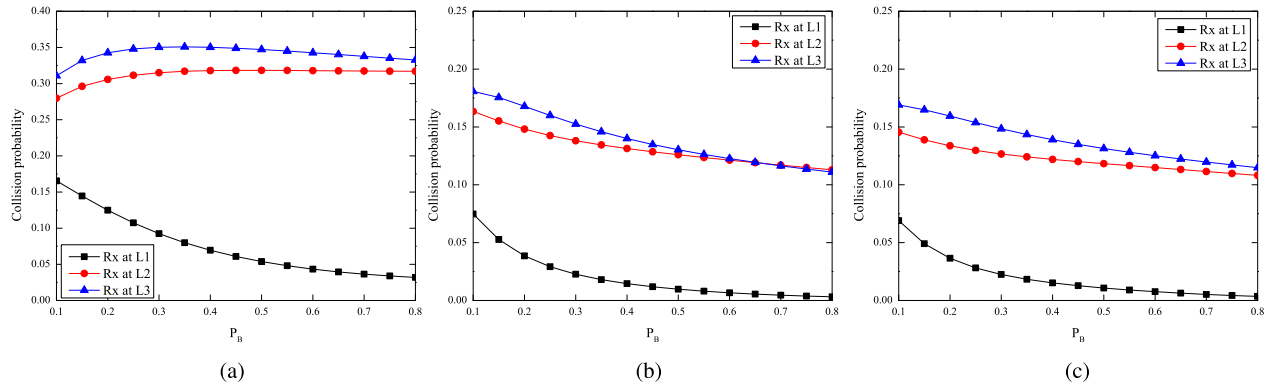

Fig. 10. Packet collision probability when Bus in lane 1. (a) Target vehicle in lane 1. (b) Target vehicle in lane 2. (c) Target vehicle in lane 3.

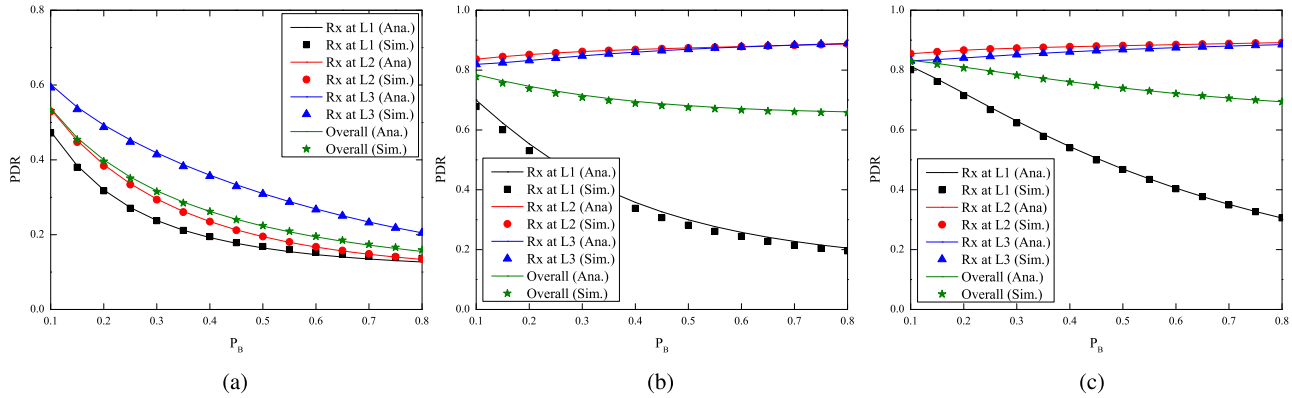

Fig. 11. Packet delivery ratio (PDR) when when the buses are located at lane 1. (a) Target vehicle in lane 1. (b) Target vehicle in lane 2. (c) Target vehicle in lane 3.

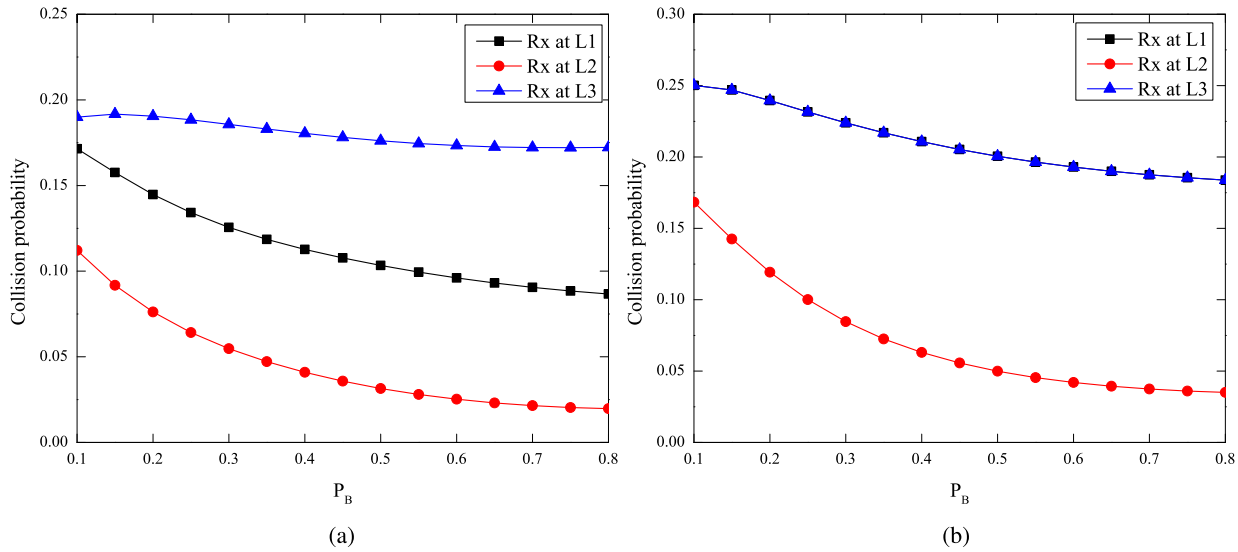

Fig. 12. Packet collision probability when when the buses are located at lane 2. (a) Tagged car at lane 1. (b) Tagged car at lane 2.

packet collision probability for a receiver in lane two due to the limited transmission range of interfering cars in lane 2. Due to the symmetry, the packet collision probabilities for a receiver in lane one and three are the same. Note that due to the symmetry, packet collision characteristics for the target vehicle in lane three will be similar to the characteristics for a target vehicle in lane one (i.e., Fig. 12a).

In Fig. 13, we present the PDRs of the target vehicle in lane one and two when the bus is assumed running in lane two. Fig. 13a illustrates the PDR when the target vehicle is in lane one. In this

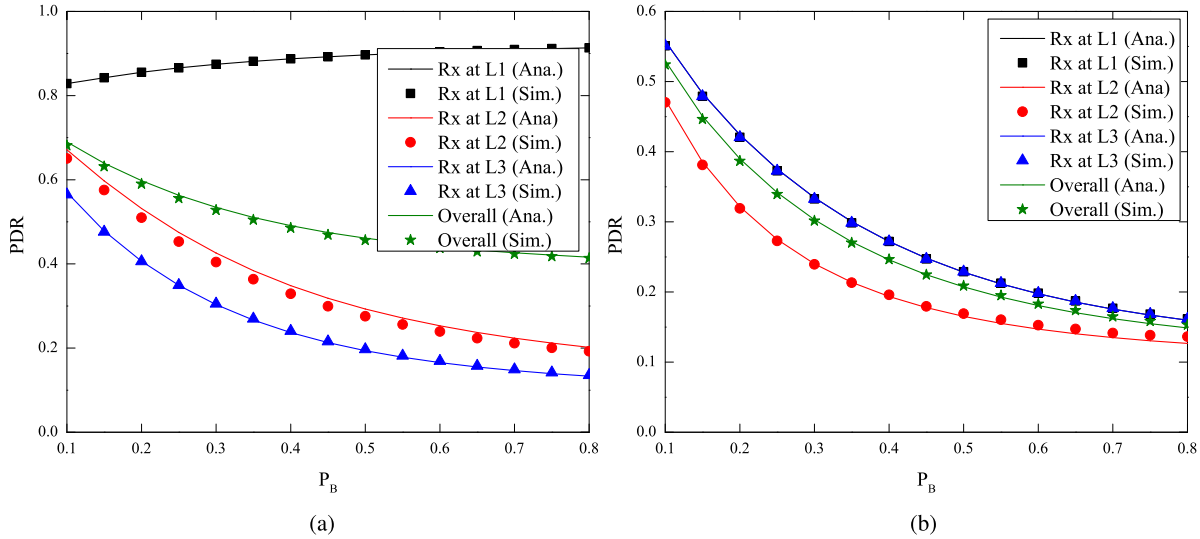

Fig. 13. Packet delivery ratio (PDR) when when the buses are located at lane 2. (a) Tagged car at lane 1. (b) Tagged car at lane 2.

scenario, the increasing of the PDR for lane one can be explained in the same way as in the discussion of the results in Fig. 11b and Fig. 11c. The PDR for lane one is as high as greater than 0.8 because both the target vehicle and the destination cars are in different lanes to the bus and do not suffer any shadowing loss as mentioned in the result of Fig. 8. The shadowing loss plays a big role in the PDRs of lane two and three where the PDRs can reduce below 0.2. The PDR result for a scenario when the target vehicle and a bus are both in lane two is shown in Fig. 13b. In this scenario, the shadowing loss dominates and causes severe degradation of the overall PDR where it varies from 0.52 to 0.18. Due to the symmetrical geography of the three lane road layout, the results when the target vehicle is in lane three are the same as the results when the target vehicle is in lane one as shown in Fig. 13a.

VI. Conclusion

In this paper, we analyze the impact of the shadowing effect of big vehicles such as trucks or buses on V2V communication. The shadowing loss of a single bus is derived from an empirical V2V channel model based on measured data. The shadowing loss caused degradation in received signal strength due to multiple buses is considered using a integrated model from the geometric and stochastic analysis. We propose a more realistic point process called hardcore repulsive Poisson Point Process to model the vehicle on the road where a vehicle has to keep a safety distance to the vehicle in front. The results of analysis show that big vehicles cast a big shadow region on the road. This shadow region varies from 50 m to nearly 450 m when the big vehicle density increases from 10% to 80% of total vehicles in one lane of the road. The big vehicle shadowing loss reduces the number of cars that can communicate with a target vehicle from about 80% to 25% or 50% of the total number of cars depending on the geometric view of the obstructions. Considering the impact of bus shadowing, we have performed packet collision analysis, where we have observed higher packet collisions in lanes without buses than in lanes with buses. In the future, we will extend our analysis to the scenario which considers big vehicles with various size. Furthermore, in a real-world scenario, the distance between vehicles may differ based on the vehicles' speed, weather condition and drivers' behavior. It will be interesting to consider the impact of big vehicles with more sophisticated distance models. Besides, we will also consider the design of the relaying mechanism which makes use of antenna(s) placed on top of the big vehicle to relay the blocked vehicular data from one side of the big vehicle to the other side.

References

[1] A. Bazzi, B. M. Masini, A. Zanella, and I. Thibault, "On the performance of IEEE 802.11p and LTE-V2V for the cooperative awareness of connected vehicles," *IEEE Trans. Veh. Technol.*, vol. 66, no. 11, pp. 10 419–10 432, Nov. 2017.

[2] H. Nguyen, M. Noor-A-Rahim, Z. Liu, D. Jamaludin, and Y. L. Guan, "A semi-empirical performance study of two-hop DSRC message relaying at road intersections," *Information*, vol. 9, no. 6, p. 147, Jun. 2018.

[3] H. Seo, K. D. Lee, S. Yasukawa, Y. Peng, and P. Sartori, "LTE evolution for vehicle-to-everything services," *IEEE Commun. Mag.*, vol. 54, no. 6, pp. 22–28, Jun. 2016.

[4] M. Noor-A-Rahim, G. G. M. N. Ali, Y. L. Guan, A. Beshah, P. H. J. Chong, and P. Dirk, "Broadcast performance analysis and improvements of the LTE-V2V autonomous mode at road intersection," *IEEE Trans. Veh. Technol.*, vol. 68, no. 10, pp. 1–1, Oct. 2019.

[5] *Dedicated Short Range Communications (DSRC) Message Set Dictionary*, SAE International Std., SAE J2735, 2016.

[6] *IEEE Standard for Information Technology– Local and Metropolitan Area Networks– Specific Requirements– Part 11: Wireless LAN Medium Access Control (MAC) and Physical Layer (PHY) Specifications Amendment 6: Wireless Access in Vehicular Environments*, IEEE Std 802.11, Jul. 2010, pp. 1–51.

[7] "Intelligent transport systems (ITS); vehicular communications; basic set of applications; part 2: Specification of cooperative awareness basic service," Draft, Tech. Rep., EN 302 637-2 V1.3.0, 2013.

[8] F. Ahmed-Zaid and A. Carter, "Vehicle safety communications project task 3 final report: Identify intelligent vehicle safety applications enabled by DSRC," Tech. Rep., DOT HS 809 859, Mar. 2005.

[9] Y. P. Fallah, C. L. Huang, R. Sengupta, and H. Krishnan, "Analysis of information dissemination in vehicular ad-hoc networks with application to cooperative vehicle safety systems," *IEEE Trans. Veh. Technol.*, vol. 60, no. 1, pp. 233–247, Jan. 2011.

[10] C. Han, M. Dianati, R. Tafazolli, R. Kernchen, and X. Shen, "Analytical study of the IEEE 802.11p MAC sublayer in vehicular networks," *IEEE Trans. Intell. Transp. Syst.*, vol. 13, no. 2, pp. 873–886, Jun. 2012.

[11] Y. Yao, L. Rao, and X. Liu, "Performance and reliability analysis of IEEE 802.11p safety communication in a highway environment," *IEEE Trans. Veh. Technol.*, vol. 62, no. 9, pp. 4198–4212, Nov. 2013.

[12] R. He, A. F. Molisch, F. Tufvesson, Z. Zhong, B. Ai, and T. Zhang, "Vehicle-to-vehicle propagation models with large vehicle obstructions," *IEEE Trans. Intell. Transp. Syst.*, vol. 15, no. 5, pp. 2237–2248, Oct. 2014.

[13] T. Abbas, K. Sjöberg, J. Karedal, and F. Tufvesson, "A measurement based shadow fading model for vehicle-to-vehicle network simulations," *Int. J. Antennas Propag.*, vol. 2015, 2015, Art. no. 190607.

[14] Y. Wang, K. Venugopal, A. F. Molisch, and R. W. Heath, "Blockage and coverage analysis with mmWave cross street BSs near urban intersections," in *Proc. IEEE Int. Conf. Commun.*, May 2017, pp. 1–6.

[15] M. G. Nilsson, D. Vlastaras, T. Abbas, B. Bergqvist, and F. Tufvesson, "On multilink shadowing effects in measured V2V channels on highway," in *Proc. 9th Eur. Conf. Antennas Propag.*, Apr. 2015, pp. 1–5.

[16] R. Meireles, M. Boban, P. Steenkiste, O. Tonguz, and J. Barros, "Experimental study on the impact of vehicular obstructions in VANETs," in *Proc. IEEE Veh. Netw. Conf*, Dec. 2010, pp. 338–345.

[17] M. Boban, T. T. V. Vinhoza, M. Ferreira, J. Barros, and O. K. Tonguz, "Impact of vehicles as obstacles in vehicular ad hoc networks," *IEEE J. Sel. Areas Commun.*, vol. 29, no. 1, pp. 15–28, Jan. 2011.

[18] M. Boban, X. Gong, and W. Xu, "Modeling the evolution of line-of-sight blockage for V2V channels," in *Proc. IEEE 84th Veh. Technol. Conf. (VTC-Fall)*, Sep. 2016, pp. 1–7.

[19] R. Huang, J. Wu, C. Long, Y. Zhu, B. Li, and Y. Lin, "Mitigate the obstructing effect of vehicles on the propagation of vanets safety-related information," *IEEE Trans. Veh. Technol.*, vol. 67, no. 7, pp. 5558–5569, Jul. 2018.

[20] K. A. Hafeez, L. Zhao, B. Ma, and J. W. Mark, "Performance analysis and enhancement of the DSRC for VANET's safety applications," *IEEE Trans. Veh. Technol.*, vol. 62, no. 7, pp. 3069–3083, Sep. 2013.

[21] K. A. Hafeez, A. Anpalagan, and L. Zhao, "Optimizing the control channel interval of the DSRC for vehicular safety applications," *IEEE Trans. Veh. Technol.*, vol. 65, no. 5, pp. 3377–3388, May 2016.

[22] H. Peng *et al.*, "Performance analysis of IEEE 802.11p DCF for multiplatooning communications with autonomous vehicles," *IEEE Trans. Veh. Technol.*, vol. 66, no. 3, pp. 2485–2498, Mar. 2017.

[23] M. Haenggi, J. G. Andrews, F. Baccelli, O. Dousse, and M. Franceschetti, "Stochastic geometry and random graphs for the analysis and design of wireless networks," *IEEE J. Sel. Areas Commun.*, vol. 27, no. 7, pp. 1029–1046, Sep. 2009.

[24] B. Matérn, *Spatial Variation*, Springer Lecture Notes in Statistics, Berlin, Germany: Springer, 1986.

[25] M. Haenggi, "Mean interference in hard-core wireless networks," *IEEE Commun. Lett.*, vol. 15, no. 8, pp. 792–794, Aug. 2011.

[26] B. Cho, K. Koufos, and R. Jantti, "Bounding the mean interference in Matérn type II hard-core wireless networks," *IEEE Wireless Commun. Lett.*, vol. 2, no. 5, pp. 563–566, Oct. 2013.

[27] J. G. Andrews, R. K. Ganti, M. Haenggi, N. Jindal, and S. Weber, "A primer on spatial modeling and analysis in wireless networks," *IEEE Commun. Mag.*, vol. 48, no. 11, pp. 156–163, Nov. 2010.

[28] N. Deng, W. Zhou, and M. Haenggi, "The Ginibre point process as a model for wireless networks with repulsion," *IEEE Trans. Wireless Commun.*, vol. 14, no. 1, pp. 107–121, Jan. 2015.

[29] H. Kong, I. Flint, P. Wang, D. Niyato, and N. Privault, "Exact performance analysis of ambient RF energy harvesting wireless sensor networks with Ginibre point process," *IEEE J. Sel. Areas Commun.*, vol. 34, no. 12, pp. 3769–3784, Dec. 2016.

[30] X. Lu, I. Flint, D. Niyato, N. Privault, and P. Wang, "Self-sustainable communications with RF energy harvesting: Ginibre point process modeling and analysis," *IEEE J. Sel. Areas Commun.*, vol. 34, no. 5, pp. 1518–1535, May 2016.

[31] C. Choi and F. Baccelli, "Poisson Cox point processes for vehicular networks," *IEEE Trans. Veh. Technol.*, vol. 67, no. 10, pp. 10 160–10 165, Oct. 2018.

[32] L. Cheng, B. E. Henty, D. D. Stancil, F. Bai, and P. Mudalige, "Mobile vehicle-to-vehicle narrow-band channel measurement and characterization of the 5.9 GHz dedicated short range communication (DSRC) frequency band," *IEEE J. Sel. Areas Commun.*, vol. 25, no. 8, pp. 1501–1516, 2007.

[33] G. M. Kizer, *Digital Microwave Communication Engineering: Engineering Point-to-Point Microwave Systems*. New York, NY, USA: Wiley-IEEE Press, 2013.

[34] K. Bullington, "Radio propagation at frequencies above 30 megacycles," *Proc. IRE*, vol. 35, no. 10, pp. 1122–1136, Oct. 1947.

[35] J. Epstein and D. W. Peterson, "An experimental study of wave propagation at 850 MC," *Proc. IRE*, vol. 41, no. 5, pp. 595–611, May 1953.

[36] J. Deygout, "Multiple knife-edge diffraction of microwaves," *IEEE Trans. Antennas Propag.*, vol. 14, no. 4, pp. 480–489, Jul. 1966.

[37] J. Deygout, "Correction factor for multiple knife-edge diffraction," *IEEE Trans. Antennas Propag.*, vol. 39, no. 8, pp. 1256–1258, Aug. 1991.

[38] ITU-R, *Propagation by Diffraction*, International Telecommunication Union Radiocommunication Sector P Series P.526-14, Feb. 2018.

[39] M. I. Hassan, H. L. Vu, and T. Sakurai, "Performance analysis of the IEEE 802.11 MAC protocol for dsrc safety applications," *IEEE Trans. Veh. Technol.*, vol. 60, no. 8, pp. 3882–3896, Oct. 2011.

[40] X. Ma and X. Chen, "Delay and broadcast reception rates of highway safety applications in vehicular ad hoc networks," in *Mobile Netw. Veh. Environ.*, May 2007, pp. 85–90.